



Loss of the major Type I arginine methyltransferase PRMT1 causes substrate scavenging by other PRMTs

Surbhi Dhar^{1*}, Vidyasiri Vemulapalli^{1*}, Alexander N. Patananan², Grace L. Huang², Alessandra Di Lorenzo¹, Stephane Richard⁴, Michael J. Comb³, Ailan Guo³, Steven G. Clarke² & Mark T. Bedford¹

¹Department of Molecular Carcinogenesis, The University of Texas MD Anderson Cancer Center, Smithville, TX 78957, USA, ²Department of Chemistry and Biochemistry, University of California Los Angeles, Los Angeles, CA 90095, USA, ³Cell Signaling Technology Inc., Danvers, MA 01923, USA, ⁴Terry Fox Molecular Oncology Group and the Bloomfield Center for Research on Aging, Lady Davis Institute for Medical Research, Sir Mortimer B. Davis Jewish General Hospital, and Departments of Medicine and Oncology, McGill University, Montréal, Québec, Canada.

Arginine methylation is a common posttranslational modification that is found on both histone and non-histone proteins. Three types of arginine methylation exist in mammalian cells: monomethylarginine (MMA), asymmetric dimethylarginine (ADMA) and symmetric dimethylarginine (SDMA). PRMT1 is the primary methyltransferase that deposits the ADMA mark, and it accounts for over 90% of this type of methylation. Here, we show that with the loss of PRMT1 activity, there are major increases in global MMA and SDMA levels, as detected by type-specific antibodies. Amino acid analysis confirms that MMA and SDMA levels accumulate when ADMA levels are reduced. These findings reveal the dynamic interplay between different arginine methylation types in the cells, and that the pre-existence of the dominant ADMA mark can block the occurrence of SDMA and MMA marks on the same substrate. This study provides clear evidence of competition for different arginine methylation types on the same substrates.

Arginine methylation is an abundant posttranslational modification (PTM), with about 0.5% of arginine residues methylated in mammalian tissues^{1,2}, and roughly 2% of arginine residues methylated in rat liver nuclei³. This common PTM has been implicated in the regulation of a large number of cellular processes⁴, and is often deregulated in cancer⁵. Three types of methylarginine species exist: ω - N^G -monomethylarginine (MMA), ω - N^G, N^G -asymmetric dimethylarginine (ADMA) and ω - N^G, N^G -symmetric dimethylarginine (SDMA). The formation of MMA, ADMA and SDMA in mammalian cells is performed by a family of nine protein arginine methyltransferases (PRMTs)⁴. PRMT1, 2, 3, 6, 8 and CARM1 (also called PRMT4) are Type I arginine methyltransferases that deposit the ADMA mark. PRMT5 is the primary Type II arginine methyltransferase that deposits the SDMA mark. PRMT7 has also been shown to display weak Type II activity, but is primarily responsible for depositing the MMA mark, thus categorizing it as a Type III enzyme⁶. PRMT9 has yet to be fully characterized.

The majority of the PRMTs methylate glycine- and arginine-rich (GAR) motifs within their substrates, a motif that supports both ADMA and SDMA marks⁷. CARM1 displays unique substrate specificity in that it does not methylate GAR motifs⁸, but rather a PGM motif, which is proline-, glycine- and methionine-rich⁹. PRMT5 can also symmetrically dimethylate arginine residues within PGM motifs⁹. Thus, CARM1 substrates (SmB, CA150, PABP, U1C and SF3B4) and PRMT1, 3, 6 and 8 substrates (GAR) can also be symmetrically methylated by PRMT5⁹. However, because these methylatable regions harbor multiple arginine residues, it is unclear if these different types of arginine methylation (ADMA and SDMA) compete for the same arginine residue(s) within GAR and PGM motifs. It is generally felt that monomethylarginine is a precursor state to ADMA and SDMA, and MMA is thus a relatively low abundant intermediate, but some Type I PRMTs may selectively monomethylate a select few substrates. Moreover, a few substrates may be heavily monomethylated due to the predominant Type III activity reported for PRMT7⁶.

To investigate the propensity of different PRMTs to mono-methylate substrates, we used a panel of methylarginine-specific antibodies that specifically detect this methyl-mark. We also used a set of PRMT knockout and knockdown cell lines to investigate which of the PRMTs (PRMT1, 3, 4, 5 and 6) are primarily responsible for depositing the MMA mark. We do not yet have a well-characterized set of PRMT7 knockout or knockdown cell

SUBJECT AREAS:

METHYLATION

HISTONE POST-TRANSLATIONAL
MODIFICATIONS

NUCLEAR RECEPTORS

GENE SILENCING

Received

28 January 2013

Accepted

31 January 2013

Published

19 February 2013

Correspondence and requests for materials should be addressed to M.T.B. (mtbedford@mdanderson.org)

* These authors contributed equally to this work.



lines, so this enzyme was not included in the screen. The MMA-specific antibodies detected a number of methylated proteins by Western analysis. Unexpectedly, we found that very few bands were lost when individual PRMTs were knocked-out or knocked-down. Even more surprising is the observation that MMA levels actually increase when PRMT1 is knocked-out. Further analysis showed that both MMA and SDMA levels are dramatically increased in PRMT1-null cells. Thus, loss of PRMT1 activity could impact substrate protein function, not by loss of methylation, but rather by switching to a different methylation type.

Results

Methyl-arginine specific antibodies reveal methylation type switching with PRMT1 loss. A panel of mono-methyl arginine antibodies was developed by Cell Signaling Technology® (CST). A GAR motif (Rme1GG) was used as the antigen to generate the MMA1 antibody, and degenerate peptide with a single fixed mono-methyl

arginine residue (Rme1XX) was used as an alternative antigen to generate the MMA2-5 antibodies. To characterize these antibodies, we tested them on total cell lysates for PRMT1 wild-type and null cells. The loss of PRMT1 is not compatible with cell viability, so we used a floxed MEF cell line that can be treated with tamoxifen (OHT) to induce PRMT1 loss (PRMT1^{fl/-} ER-Cre MEFs)¹⁰. The cell lysates are harvested eight-days after OHT-treatment, which is a few days (2–4 days) prior to cell death. PRMT1 has long been known to generate MMA and ADMA marks *in vitro*¹¹. We anticipated that in cells, certain PRMT1 substrates would be monomethylated and others would be dimethylated, and that both types of methylation would be lost with PRMT1 removal. Unexpectedly, we observed an increase of immune-reactivity with all five different MMA antibodies upon loss of PRMT1 activity (Fig. 1A). We expanded this study using cell lysates from knockout PRMT3, CARM1 and PRMT6 cells (Fig. 1B–D). The phenomenon of massive MMA increase was not observed with the loss of these other three PRMTs. We next

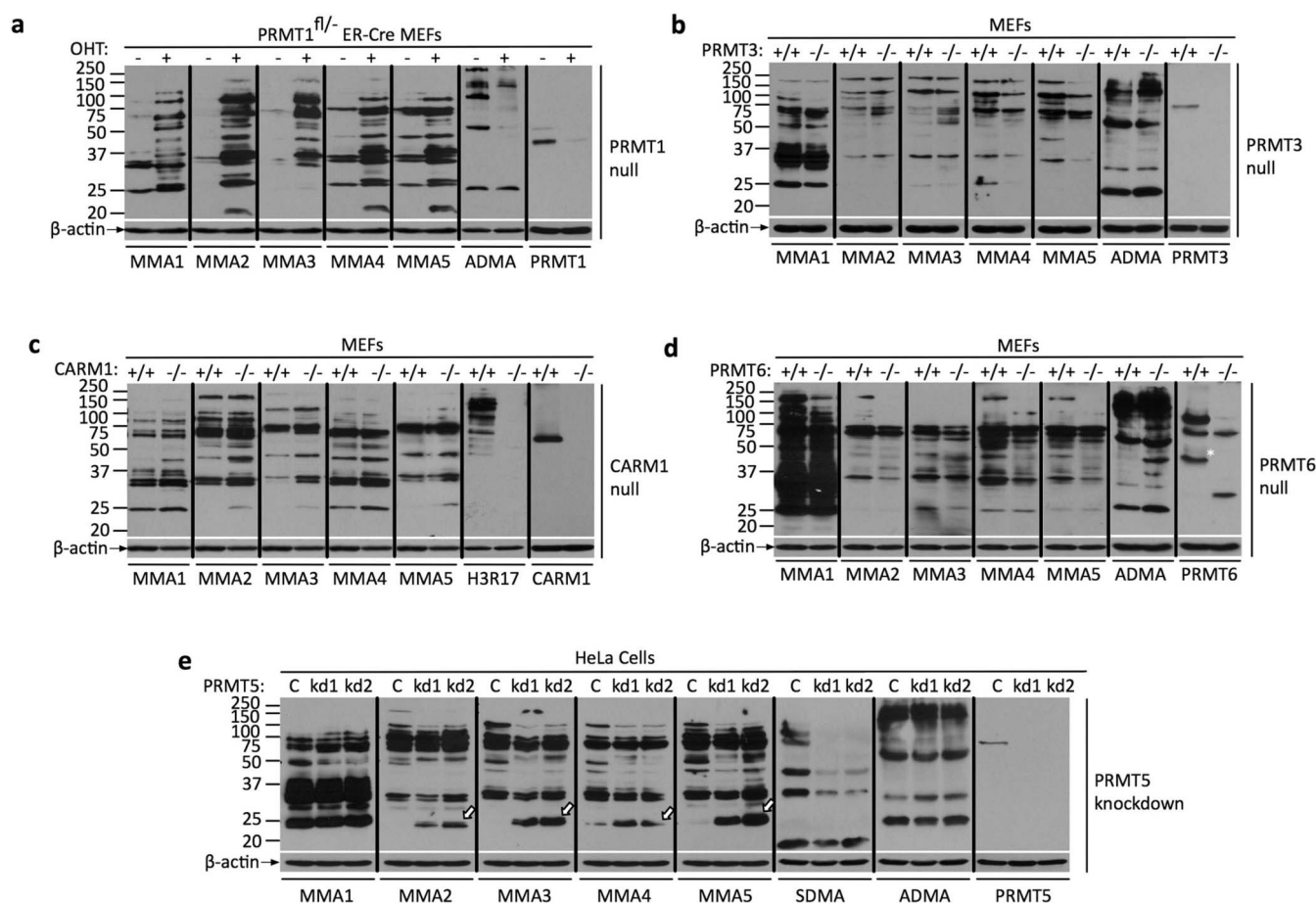


Figure 1 | Characterization of the monomethylarginine antibodies. (a) PRMT1^{fl/-} ER-Cre MEFs were untreated or treated with 4-hydroxytamoxifen (OHT) for 8 days. Whole cell lysates were prepared and immunoblotted with monomethylarginine (MMA1–5) and asymmetric dimethylarginine (ADMA) antibodies. MMA antibodies are highly immunoreactive towards PRMT1 knockout (–/–) MEFs compared to the wild-type (+/+) counterparts suggesting that the KO cells have a rich pool of mono-methylated proteins. ADMA antibody showed reduced immunoreactivity in PRMT1 –/– cells, which suggests that they have lower levels of dimethylated proteins. Whole cell extracts of PRMT3 (b), CARM1 (c) and PRMT6 (d) +/+ and –/– MEFs were prepared and immunoblotted with MMA1–5 antibodies. The immunoreactivity patterns are the same in +/+ versus –/– cells. PRMT3 (b), PRMT5 (e) and PRMT6 (d) MEFs were also blotted with ADMA antibody, revealing no changes in banding patterns. CARM1 (c) MEFs were immunoblotted with H3R17 antibody (H3R17me2a, Millipore). Although this antibody was originally generated to recognize dimethyl-Arg17 on histone H3, it was shown to behave as a pan-antibody⁹. (c) It recognized a number of proteins in +/+ cells that are absent in CARM1 –/– cells, suggesting a decrease of dimethylation in these cells. (e) PRMT5 control and knockdown (KD) HeLa cells were immunoblotted with MMA1–5 and symmetric dimethylarginine (SDMA) antibodies. MMA antibodies do not show significant differences in band patterns in control versus KD cells except for a doublet of bands, which appeared at 25 kDa in KD cells (indicated with solid white arrows). SDMA antibody showed reduced immunoreactivity in KD cells. Western analyses with α PRMT1 (a), α PRMT3 (b), α CARM1 (c), α PRMT5 (e) and α PRMT6 (marked with asterisk) (d) antibodies show the loss of these PRMTs in the respective –/– cell lines. All lysates were blotted with β -actin antibody to visualize equivalent loading.



investigated the effect of PRMT5 knock-down on MMA levels (Fig. 1E). Again, we did not see the large-scale generation of monomethylated substrates with the reduction of PRMT5 levels. However, there is one protein that migrates at 25kDa and becomes monomethylated with PRMT5 knock-down. Thus, the loss of PRMT1 activity seems unique in its ability to facilitate the wholesale generation of monomethylated substrates.

MMA and SDMA levels reach a maximum within 4–6 days after PRMT1 loss. Next, we investigated the dynamics of ADMA loss and MMA gain, after PRMT1 removal. This experiment was again facilitated by the availability of the PRMT1^{fl/-} ER-Cre MEFs. Once these cells are treated with 4-hydroxytamoxifen (OHT), the Cre activity is translocated into the nucleus where it removes the floxed PRMT1 allele. The cellular PRMT1 protein levels immediately begin to drop, and by day-2 trace amounts of PRMT1 are seen, with no PRMT1 protein observed by day-4 post OHT-treatment (Fig. 2C, middle panel). Concomitant with PRMT1 protein loss, we observe an increase in MMA levels (Fig. 2A) along with the expected loss of ADMA levels (Fig. 2B). After an initial dramatic loss of ADMA

levels we see some compensation, as well as novel substrate methylation, which begins at day-4 post PRMT1 loss. This could be due to the cell attempting to compensate for PRMT1-loss with the overexpression of other PRMTs. We thus tested the expression levels of CARM1 and PRMT3, 5, 6, 7 at four- and eight-days after PRMT1 removal (Supplemental Fig. 1). At the 4-day time-point, we do not observe any major increase in the protein levels of these five PRMTs. However, on the 8th day we do see an attempt made by the cells to compensate for PRMT1 loss by elevating PRMT6 and PRMT7 levels, and we also see streaking of CARM1 by Western analysis, perhaps signifying hyper protein modification. It is important to note that while we do not see any PRMT expression level compensation at day-4 we do see a dramatic increase in MMA levels at this time point, indicating that this increase in MMA levels is not linked to the overexpression of the tested PRMTs (although not all PRMTs were tested). We also evaluated SDMA level changes during the 10-day period after PRMT1 removal and noted a significant increase in symmetrical dimethylation that accompanies MMA increase, after PRMT1 loss (Fig. 2C).

Amino acid analysis confirms the global accumulation of MMA and SDMA levels with PRMT1 loss. To independently confirm the dramatic elevation of cellular MMA and SDMA levels observed in PRMT1-deficient cells using antibodies (Fig. 1 and Fig. 2), we isolated and acid hydrolyzed proteins from PRMT1 wild-type and PRMT1^{fl/-} ER-Cre MEFs treated with tamoxifen for 7 days. To quantitate methylated arginine residues in MEFs, we developed a novel two-dimensional approach that takes advantage of the high resolution of cation-exchange and reverse-phase columns coupled to the sensitivity of the fluorescence labeling (Fig. 3 and Supplemental Fig. 4). PRMT1 wild-type or knockout acid hydrolysates were first separated by high-resolution cation exchange chromatography. The fractions obtained were then labeled with *o*-phthalaldehyde (OPA) to enable the detection of picomole levels of amino acids after a second step of separation using two conditions of reverse-phase HPLC to quantitate MMA, SDMA, and ADMA relative to the level of arginine (Supplemental Fig. 5).

We found that MMA levels increased almost five-fold in the PRMT1 knockout cells compared to wild type cells (Table 1). Additionally, we found that the level of SDMA was also increased almost 3-fold in the PRMT1 knockout cells (Table 1). These results support the conclusion from the antibody studies that both MMA and SDMA levels rise with the loss of the major protein arginine methyltransferase. As a control, we measured the level of ADMA residues and found a 50% reduction in the PRMT1 knockout cells as would be expected from the loss of a major type I PRMT (Table 1). These results also demonstrate the prevalence of protein arginine methylation in MEF proteins. We find about 0.4 residues of ADMA per 100 arginine residues; the levels of MMA are roughly 35-fold lower and SDMA levels are about 10-fold lower. Thus, ADMA is the predominant methylated arginine residue in MEFs. The levels we have observed here in wild-type MEFs are comparable to those previously shown for rat brain and liver (Supplemental Table 1). The content of ADMA and SDMA is similar in MEFs and rat brain and liver, whereas the levels of MMA are significantly lower in MEFs. We note that in the subfraction of nuclear proteins, ADMA levels may reach 1 to 2% of arginine residues¹⁻³. The compensatory increases in MMA and SDMA levels seen here in PRMT1 knockout MEFs supports the hypothesis that ADMA marks play a key role in the interplay of global arginine methylation events.

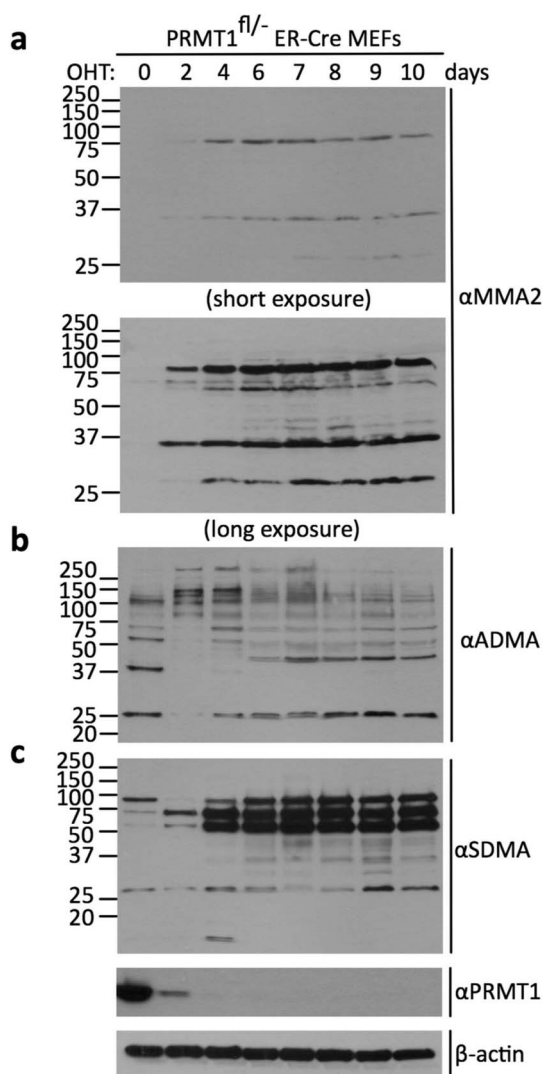


Figure 2 | Arginine methylation trends in inducible PRMT1-knockout MEFs. PRMT1^{fl/-} ER-Cre MEFs were untreated or treated with 4-hydroxytamoxifen (OHT) for 10 days. Total cell lysates from different days of treatment were immunoblotted with antibodies against monomethylarginine (MMA2) (a), asymmetric dimethylarginine (ADMA) (b), symmetric dimethylarginine (SDMA), PRMT1 and β -actin (c).

Discussion

Classic studies in the protein methylation field have estimated the ratios of the different types of arginine methylation across a large number of tissue and cell types to be roughly as follows – 1500:3:2:1 for Arg:ADMA:MMA:SDMA^{1,2}. We have found that

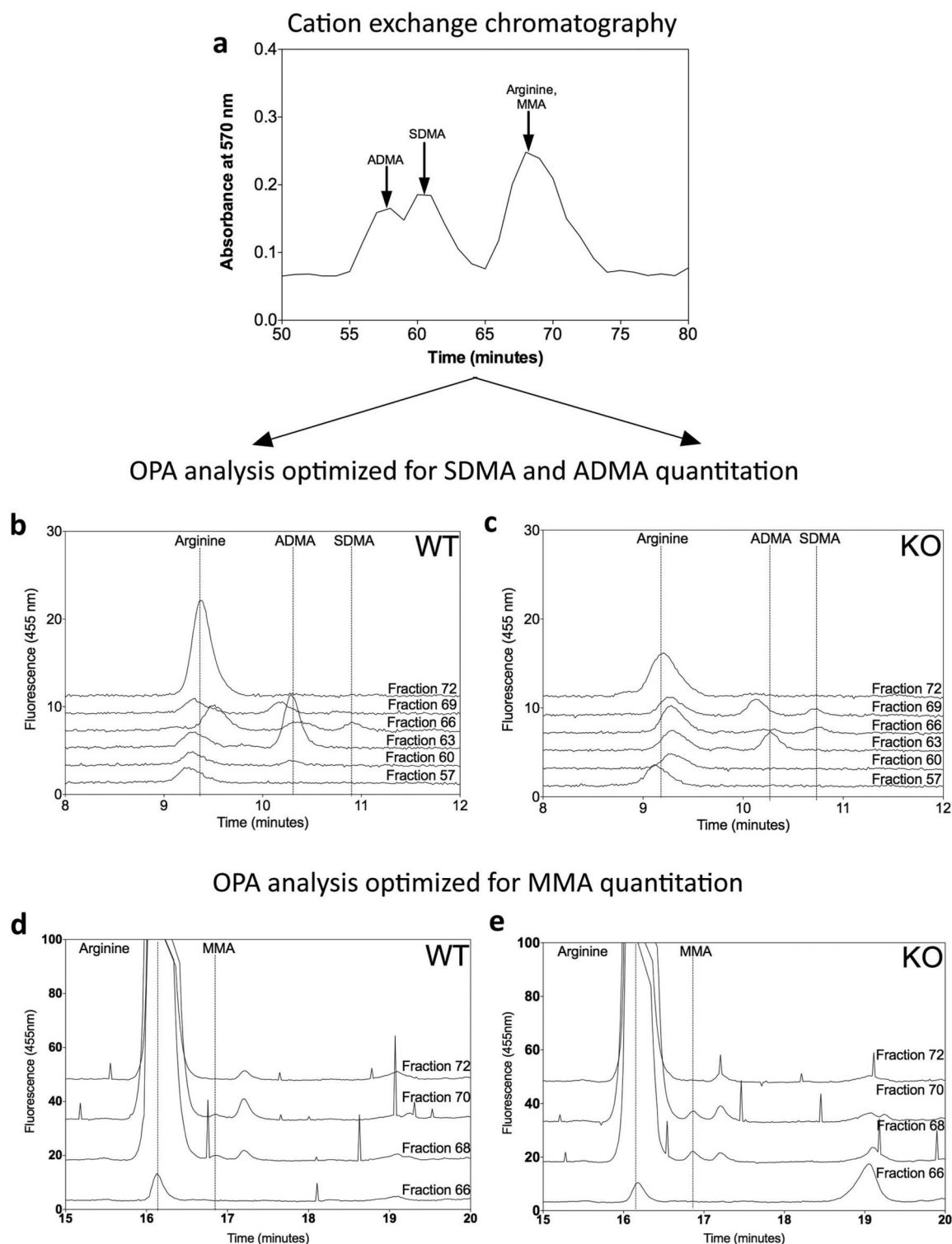


Figure 3 | Quantification of MMA, ADMA, SDMA, and arginine levels in protein hydrolysates of wild-type and PRMT1-knockout MEFs. Cell pellets from PRMT1 wild-type and knockout MEFs were acid hydrolyzed and the resulting amino acids separated by high-resolution cation exchange chromatography as described in "Methods". The separation of standards (1 μmol) of ADMA, SDMA, and MMA/arginine with ninhydrin detection as described by Zurita-Lopez *et al.* (2012)⁹ is shown in the control chromatograph (a). The separation of these amino acids is typical, although small changes in the elution times can occur between runs. Cell hydrolysates were then chromatographed without standard amino acids and fractions analyzed by reverse-phase HPLC after derivatization with OPA for fluorescence quantitation as described in "Methods". HPLC conditions were optimized to separate the large pool of arginine from ADMA and SDMA in wild-type (b) and PRMT1 knockout (c) and from MMA in wild-type (d) and PRMT1 knockout (e) samples (Supplemental Fig. 5). The total amount of a given species was quantified by summing the integrated area under the curve for all HPLC fractions containing the respective species that are consistent with the migration on the cation-exchange column.



Table 1 | Quantitation of MMA, ADMA, and SDMA in wild-type and PRMT1 knockout MEF protein hydrolysates. The number of residues of methylated arginine derivatives per 1000 residues of arginine is shown

Residue analyzed	Experiment #	PRMT1 WT	PRMT1 KO	Average fold change (KO to WT)
		Residues per 1000 arginine residues		
MMA	Experiment 1	0.16	0.83	4.73
	Experiment 2	0.07	0.30	
ADMA	Experiment 1	4.36	3.14	0.52
	Experiment 2	3.69	1.76	
	Experiment 3	3.98	1.49	
SDMA	Experiment 1	0.34	0.94	2.76

once PRMT1 activity is removed there is a large increase in global levels of both MMA and SDMA, and consequently a major realignment of these ratios. This is likely due to the fact that PRMT1 is the primary type I enzyme, accounting for about 90% of global ADMA deposition¹². This dominant activity of PRMT1 seems to keep the other PRMTs in check. With the loss of PRMT1, a large number of substrates become targets for Type II and III PRMTs, because these substrates are presumably no longer blocked by an ADMA modification. It is well established that the same arginine residues can be targeted by both Type I and Type II PRMTs, especially in the context of histone tail methylation¹³, but the extent of this competition was unappreciated until now.

We considered the possibility that PRMT1 may be complexed with another PRMT, which may deposit a MMA mark and act as a priming enzyme for PRMT1. In this scenario, with PRMT1 removal the priming enzyme would still monomethylate substrates, but these substrates would never be further converted to an ADMA state. This could account for the dramatic increase in MMA levels after PRMT1 knock-out. To investigate this possibility we transfected cells with a set of GFP-PRMTs and performed a GFP immunoprecipitation followed by anti-PRMT1 Western analysis (Supplemental Fig. 2). Only GFP-PRMT1 and GFP-PRMT8 (a brain specific enzyme¹⁴) could immunoprecipitate endogenous PRMT1, suggesting that there is not a common priming PRMT, which is complexed with PRMT1.

Only with the loss of PRMT1 activity, and not with the loss of other PRMTs, do we see massive increases of MMA levels (Fig. 1A). However, with reduced PRMT5 activity, we observe an increase in the MMA state of a single protein that migrates at 25 kDa (Fig. 1E – arrow-head). This is the size of the splicing factor SmB, which is a well-characterized PRMT5 substrate¹⁵. By immunoprecipitation of SmB, from wild-type and PRMT5 knock-down cells, we confirmed that SmB does indeed become monomethylated when PRMT5 levels are reduced (Supplemental Fig. 3). It is important to note that the PRMT5 knock-down is very efficient (Fig. 1E), although likely not complete. Thus, low levels of PRMT5 may remain in the knock-down cell, and because PRMT5 displays a nonprocessive enzymatic mechanism¹⁶, these low levels of PRMT5 will find unmethylated SmB substrate for the first monomethylation reaction, but after release, will more likely find another unmethylated substrate, rather than a MMA substrate for conversion to a SDMA substrate. Thus, there will be an accumulation of SmB decorated with a MMA mark. This explanation will not account for the increase in MMA levels in the PRMT1 knockout cells for two reasons. First, PRMT1 is totally knocked out in these cells, and after the endogenous PRMT1 turns over there will be no enzyme present in the cells. Second, in contrast to the nonprocessive enzymatic mechanism of PRMT5¹⁶, PRMT1 is partially processive¹⁷.

Finally, it is clear that by using a combination of PRMT1^{fl/fl} ER-Cre MEF cells and MMA-specific antibodies, a large number of PRMT1 substrates can be unmasked. Thus, it will be of great value to perform large-scale IP/MS (immunoprecipitation followed by mass spectrometry) experiments to identify these PRMT1 substrates.

These additional tools will help us gain a better understanding of the diverse biological functions of the PRMTs.

Methods

Antibodies. A panel of five different rabbit monoclonal antibodies was generated to recognize proteins when monomethylated at arginine residues. MMA1 (Antibody# D5A12A3) was raised against an arginine-glycine-glycine motif, monomethylated at arginine residue (XXXRme1GGXXX and called Rme1GG). MMA2-5 (Antibody# D3C4A6, D2F4E5, D1C6D1 and D7B7F1) antibodies were generated against a peptide library containing monomethylarginine surrounded by degenerate amino acids (XXXRmeXXX and called Rme1XX). Asymmetric dimethylarginine (ADMA or Antibody# BL8241) and symmetric dimethylarginine (SDMA or Antibody# BL8243) antibodies are rabbit polyclonal antibodies, which were generated against degenerate peptides containing four asymmetric or symmetric dimethylarginine residue (XXXRme2aXXXRme2aXXXXRme2aXXXXRme2aX, and XXXRme2sGRme2sGGXXXRme2sGXXXRme2sXX respectively). All the above-mentioned antibodies were generated by Cell Signaling Technology® (CST). MMA1 is commercially available under the name Mono-Methyl Arginine, D5A12 (CST, Catalog # 8711). MMA2-5 antibodies are pooled together and available as Mono-Methyl Arginine, Me-R¹-100 (CST, Catalog # 8015). ADMA and SDMA antibodies are not yet commercially released. Y12 antibody was a gift from Robin Reed (Harvard Medical School). PRMT7 antibody was a gift from Said Sif (Ohio State University). PRMT1 antibody was a gift from Stephane Richard (McGill University). PRMT3 antibody was generated in the Bedford laboratory¹⁸. The following antibodies were obtained commercially: α H3R17me2a (Millipore), CARM1 (Bethyl), PRMT6 (Bethyl) and PRMT5 (Active Motif). The details of all the antibodies used in this study are shown in Supplementary Table 2.

Plasmids and cell lines. The generation of GFP-PRMT1-6 (Frankel *et al.*, 2002) and GFP-PRMT8 (Lee *et al.*, 2005) constructs has been described previously. GFP-PRMT7 and GFP-PRMT9 constructs were generated by cloning the human PRMT7 or PRMT9 cDNA into pEGFP-C1 (Clontech) vectors. The CARM1^{-/-} MEF line has been described previously¹⁹. The tamoxifen-inducible PRMT1^{fl/fl} ER-Cre MEF line has been described previously¹⁰. These MEFs were treated with 2 mM 4-hydroxytamoxifen, which stabilizes ER^{*}-Cre (an estrogen receptor Cre recombinase fusion) and translocates it to the nucleus, which then excises the floxed *prmt1* allele to generate PRMT1 KO MEFs. The PRMT3^{-/-} MEF line has been described previously¹⁸. The PRMT6^{-/-} MEF line was created by immortalizing MEFs from PRMT6-null embryos, according to standard 3T3 protocol²⁰. PRMT5 stable knockdown HeLa cell lines were a gift from Sharon Dent²¹. All cell lines were maintained in Dulbecco modified Eagle medium containing 10% fetal bovine serum. PRMT1 MEFs were supplemented with 3 mg/ml blasticidin, and PRMT5 KD cells were supplemented with 5 mg/ml puromycin.

Co-immunoprecipitation and western blotting. HEK293 cells were transiently transfected with expression vectors encoding GFP-PRMT (1–9) fusion proteins using Lipofectamine 2000 (Invitrogen) according to the manufacturer's instructions. Cells were harvested 30 h after transfection and whole cell extracts were prepared in mild lysis buffer (150 mM NaCl, 5 mM EDTA, 1% Triton X-100, and 10 mM Tris/HCl [pH 7.5]). The lysates were incubated with GFP antibody (Life technologies) overnight at 4°C, followed by incubation with Protein A/G beads (Thermo Scientific) for 1 h. The beads were washed three times with lysis buffer and boiled in loading buffer to elute bound proteins.

The immunoprecipitated samples or whole cell extracts were separated by SDS-PAGE and transferred onto PVDF membranes. Blots were blocked in PBS-Tween 20 containing 5% nonfat dry milk and then incubated with the appropriate primary antibody in the blocking buffer overnight at 4°C. The blots were then washed, probed with an HRP-labeled secondary antibody (or HRP-labeled protein A) and detected using enhanced chemiluminescence (Amersham).

Amino acid analysis of protein hydrolysates and quantitation of MMA, ADMA, SDMA, and arginine. 35–180 mg of wet weight packed MEFs and 100 μ L of 6 N HCl were added to a 6 \times 50-mm glass tube. Hydrolysis was carried out in a Waters



Pico-Tag Vapor-Phase apparatus in a vacuum vial with an additional 200 μL of 6 N HCl for 18 h at 110°C. After hydrolysates were vacuum dried, resuspended in 100 μL of water, and centrifuged to remove any debris, 75 μL was added to 250 μL of citrate buffer (0.2 M Na⁺, pH 2.2) and loaded onto a 0.9 \times 8 cm column of PA-35 sulfonated polystyrene beads (6–12 μm , Benson Polymeric Inc., Sparks, NV). The column was equilibrated and eluted with citrate buffer (0.35 M Na⁺, pH 5.27) at 55°C and a flow rate of 1 mL/min. Individual fractions from 50 to 80 min that included the known elution positions of ADMA, SDMA, MMA, and arginine were then derivatized with OPA for fluorescence detection after separation on reverse-phase HPLC.

Amino acids were labeled with OPA by mixing 60 μL of 1 mL cation exchange column fraction with 20 μL of 0.4 M potassium borate (pH 10.3), and 10 μL of OPA reagent (10 mg/mL OPA powder (Sigma, P0657) in 900 μL methanol, 100 μL 0.4 M potassium borate (pH 10.3), and 10 μL β -mercaptoethanol). After incubating the mixture at room temperature for 200 s, 5 μL of 0.75 M HCl was added and the sample was vortexed by hand for 5 s. The resulting fluorescent isoindole derivatives were separated and quantified using reverse-phase HPLC (HP 1090 II liquid chromatograph coupled to a Gilson Model 121 fluorometer with excitation and emission filters of 305–395 nm and 430–470 nm, respectively, and a setting of 0.01 RFU). An Alltech Adsorbosphere OPA HR (5 μm , 4.6-mm inner diameter, 250-mm length) was used with 90 μL sample injection volumes at room temperature and a flow rate of 1.5 ml/min. Solvent A consisted of 50 mM sodium acetate, pH 7.0, and solvent B of 100% methanol. Two HPLC gradients were used to optimize the quantification of MMA, ADMA, and SDMA (Supplemental Fig. 5). In situations where the fluorometer was overloaded with too much sample, such as in the case of some fractions associated with the arginine peak, a 1000-fold dilution of the cation exchange fraction was made in pH 5.27 sodium citrate buffer. Methylated arginine species were detected based on the HPLC retention time for standards and were confirmed by spiking the appropriate standard to the sample. Graphpad was used to calculate the area under the curve for the amino acid of interest. The total amount of a certain amino acid was calculated by summing every cation exchange fraction's HPLC run that had the appropriate peak present.

- Matsuoka, M. [Epsilon-N-methylated lysine and guanidine-N-methylated arginine of proteins. 3. Presence and distribution in nature and mammals]. *Seikagaku* **44**, 364–70 (1972).
- Paik, W. K. & Kim, S. Natural occurrence of various methylated amino acid derivatives. (ed. Meister, A.) (John Wiley & sons, New York, 1980).
- Boffa, L. C., Karn, J., Vidali, G. & Allfrey, V. G. Distribution of NG, NG-dimethylarginine in nuclear protein fractions. *Biochem Biophys Res Commun* **74**, 969–76 (1977).
- Bedford, M. T. & Clarke, S. G. Protein arginine methylation in mammals: who, what, and why. *Mol Cell* **33**, 1–13 (2009).
- Yang, Y. & Bedford, M. T. Protein arginine methyltransferases and cancer. *Nat Rev Cancer* **13**, 37–50 (2013).
- Zurita-Lopez, C. I., Sandberg, T., Kelly, R. & Clarke, S. G. Human protein arginine methyltransferase 7 (PRMT7) is a type III enzyme forming omega-NG-monomethylated arginine residues. *J Biol Chem* **287**, 7859–70 (2012).
- Branscombe, T. L. *et al.* Prmt5 (janus kinase-binding protein 1) catalyzes the formation of symmetric dimethylarginine residues in proteins. *J Biol Chem* **276**, 32971–6 (2001).
- Lee, J. & Bedford, M. T. PABP1 identified as an arginine methyltransferase substrate using high-density protein arrays. *EMBO Rep* **3**, 268–73 (2002).
- Cheng, D., Cote, J., Shaaban, S. & Bedford, M. T. The arginine methyltransferase CARM1 regulates the coupling of transcription and mRNA processing. *Mol Cell* **25**, 71–83 (2007).
- Yu, Z., Chen, T., Hebert, J., Li, E. & Richard, S. A mouse PRMT1 null allele defines an essential role for arginine methylation in genome maintenance and cell proliferation. *Mol Cell Biol* **29**, 2982–96 (2009).
- Lin, W. J., Gary, J. D., Yang, M. C., Clarke, S. & Herschman, H. R. The mammalian immediate-early TIS21 protein and the leukemia-associated BTG1 protein interact with a protein-arginine N-methyltransferase. *J Biol Chem* **271**, 15034–44 (1996).
- Tang, J. *et al.* PRMT1 is the predominant type I protein arginine methyltransferase in mammalian cells. *J Biol Chem* **275**, 7723–30 (2000).
- Di Lorenzo, A. & Bedford, M. T. Histone arginine methylation. *FEBS Lett* **585**, 2024–31 (2011).
- Lee, J., Sayegh, J., Daniel, J., Clarke, S. & Bedford, M. T. PRMT8, a new membrane-bound tissue-specific member of the protein arginine methyltransferase family. *J Biol Chem* **280**, 32890–6 (2005).
- Pesiridis, G. S., Diamond, E. & Van Duyn, G. D. Role of pICln in methylation of Sm proteins by PRMT5. *J Biol Chem* **284**, 21347–59 (2009).
- Antonyssamy, S. *et al.* Crystal structure of the human PRMT5:MEP50 complex. *Proc Natl Acad Sci U S A* **109**, 17960–5 (2012).
- Obianyo, O., Osborne, T. C. & Thompson, P. R. Kinetic mechanism of protein arginine methyltransferase 1. *Biochemistry* **47**, 10420–7 (2008).
- Swiercz, R., Person, M. D. & Bedford, M. T. Ribosomal protein S2 is a substrate for mammalian PRMT3 (protein arginine methyltransferase 3). *Biochem J* **386**, 85–91 (2005).
- Yadav, N. *et al.* Specific protein methylation defects and gene expression perturbations in coactivator-associated arginine methyltransferase 1-deficient mice. *Proc Natl Acad Sci U S A* **100**, 6464–8 (2003).
- Neault, M., Mallette, F. A., Vogel, G., Michaud-Levesque, J. & Richard, S. Ablation of PRMT6 reveals a role as a negative transcriptional regulator of the p53 tumor suppressor. *Nucleic Acids Res* **40**, 9513–21 (2012).
- Butler, J. S., Zurita-Lopez, C. I., Clarke, S. G., Bedford, M. T. & Dent, S. Y. Protein-arginine methyltransferase 1 (PRMT1) methylates Ash2L, a shared component of mammalian histone H3K4 methyltransferase complexes. *J Biol Chem* **286**, 12234–44 (2011).

Acknowledgements

MT Bedford is supported by CPRIT funding (RP110471) and a NIH grant (DK062248). SG Clarke is supported by NIH grant GM026020. We thank Cecilia Zurita-Lopez and Keith Stabe for their help with amino acid analysis. AN Patananan and GL Huang were supported by Ruth L. Kirschstein National Research Service Award GM007185.

Author contributions

S.D. performed the experiments depicted in Figures 2, S1 and S2. V.V. performed the experiments depicted in Figures 1 and S3, and she assembled Table S2. A.N.P., G.L.H. and S.G.C. performed the experiments depicted in Figures 3, S4 and S5, as well as Table 1 and S1. A.Di.L. generate the PRMT1 null cell lysates that were used for the amino acid analysis. S.R. generated the PRMT1 conditional K.O. cell line and PRMT6 null MEFs. M.J.C. and A.G. generated and characterized the C.S.T. antibodies that were used in this study and listed in Table S2. M.T.B. wrote the main manuscript text. All authors reviewed the manuscript.

Additional information

Supplementary information accompanies this paper at <http://www.nature.com/scientificreports>

Competing financial interests: MTB is a cofounder of EpiCypher. MJC and AG work at Cell Signaling Technology Inc.

License: This work is licensed under a Creative Commons Attribution-NonCommercial-NoDerivs 3.0 Unported License. To view a copy of this license, visit <http://creativecommons.org/licenses/by-nc-nd/3.0/>

How to cite this article: Dhar, S. *et al.* Loss of the major Type I arginine methyltransferase PRMT1 causes substrate scavenging by other PRMTs. *Sci. Rep.* **3**, 1311; DOI:10.1038/srep01311 (2013).

Loss of the major Type I arginine methyltransferase PRMT1 causes substrate scavenging by other PRMTs

Surbhi Dhar^{1^}, Vidyasiri Vemulapalli^{1^}, Alexander N. Patananan², Grace Huang², Alessandra Di Lorenzo¹, Stephane Richard⁴, Michael J. Comb³, Ailan Guo³, Steven G. Clarke², Mark T. Bedford^{1*}

¹Department of Molecular Carcinogenesis, The University of Texas MD Anderson Cancer Center, Smithville, TX 78957, USA.

²Department of Chemistry and Biochemistry, University of California Los Angeles, Los Angeles, CA 90095, USA.

³Cell Signaling Technology Inc., Danvers, MA 01923, USA.

⁴Terry Fox Molecular Oncology Group and the Bloomfield Center for Research on Aging, Lady Davis Institute for Medical Research, Sir Mortimer B. Davis Jewish General Hospital, and Departments of Medicine and Oncology, McGill University, Montréal, Québec, Canada

*Correspondence should be addressed to M.T.B. (mtbedford@mdanderson.org)

[^]Equal contribution

SUPPLEMENTAL INFORMATION

Supplemental Figure 1 – Expression analysis of PRMTs in the absence of PRMT1

Supplemental Figure 2 – Co-immunoprecipitation of GFP-PRMTs with endogenous PRMT1

Supplemental Figure 3 – Hyper-monomethylation of SmB/SmB' upon PRMT5 loss

Supplemental Figure 4 – Workflow for the two-dimensional quantification of arginine methylation

Supplemental Figure 5 – Reverse-phase HPLC methods optimized to quantify OPA-derivatives

Supplemental Table 1 – Comparison of the relative levels of MMA, ADMA, and SDMA

Supplemental Table 2 – Antibodies used in this study

Figure S1. Expression analysis of PRMTs in the absence of PRMT1. PRMT1^{fl/-} ER-Cre MEFs were untreated or treated with 4-hydroxytamoxifen (OHT) for 4 and 8 days. Whole cell extracts were prepared and subjected to Western analysis with α PRMT1, α PRMT3, α PRMT4, α PRMT5, α PRMT6, α PRMT7 and MMA1 antibodies. The β -actin control is shown for equal loading.

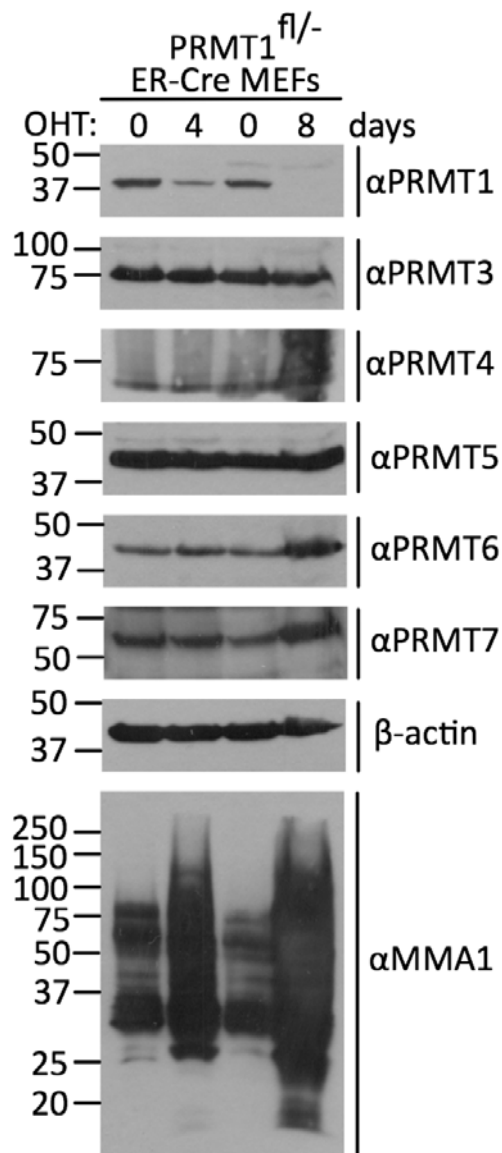


Figure S2. Co-immunoprecipitation of GFP-PRMTs with endogenous PRMT1. HEK293 cells transiently expressing GFP or GFP-PRMT [1-9] fusion proteins were immunoprecipitated with anti-GFP or anti-IgG antibodies and subjected to Western analysis with α PRMT1 (a) or α GFP (b) antibodies. PRMT1 co-immunoprecipitates with itself and with PRMT8 (indicated with solid white dots). (c) Western analysis of the input samples using α GFP antibody shows the expression of GFP-PRMT [1-9] fusion proteins, which are marked with solid white dots.

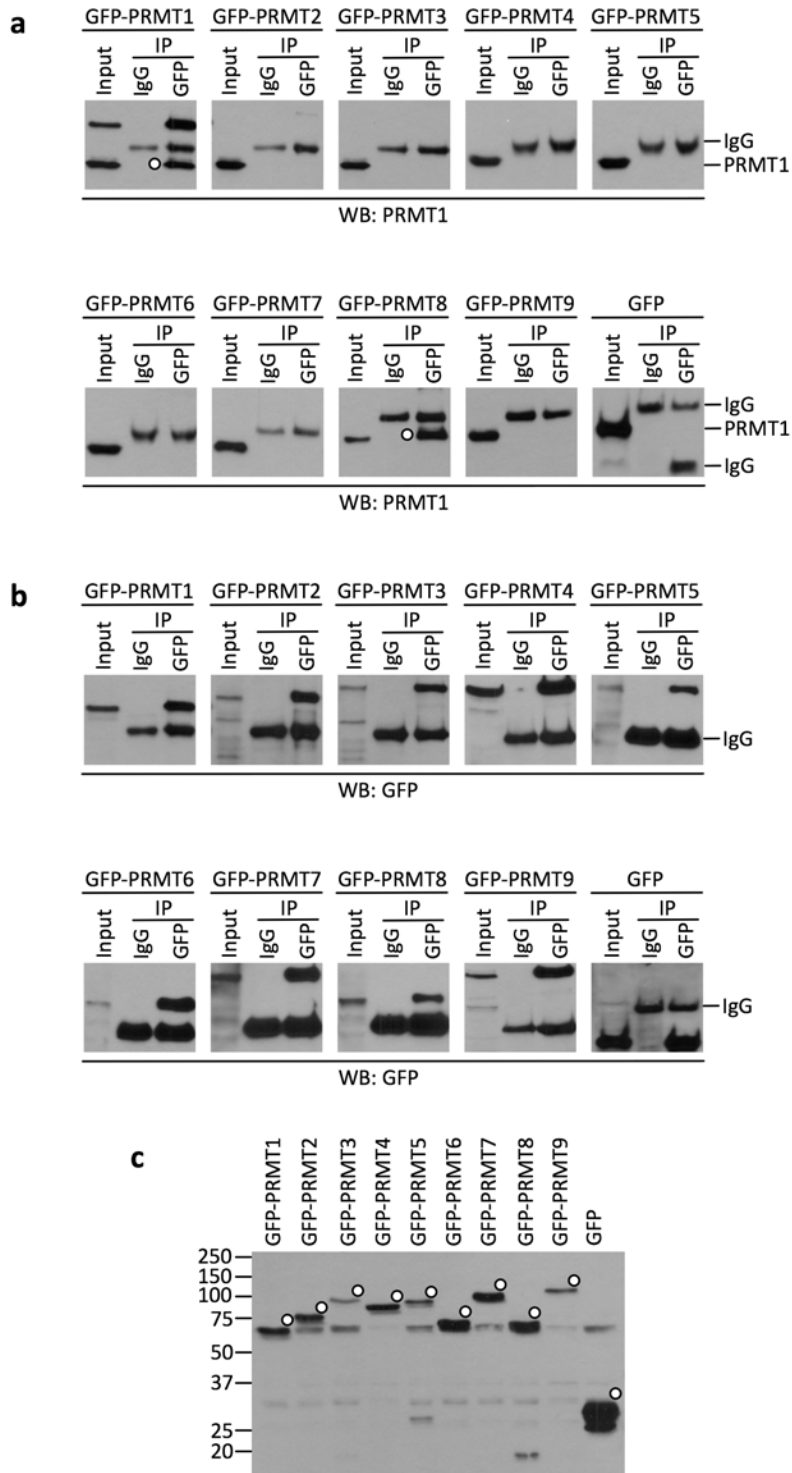


Figure S3. Hyper-monomethylation of SmB/SmB' upon PRMT5 loss. PRMT5 control and knockdown HeLa cells were immunoprecipitated (IP) with Y12 antibody and subjected to Western analysis with monomethylarginine (MMA5) antibody.

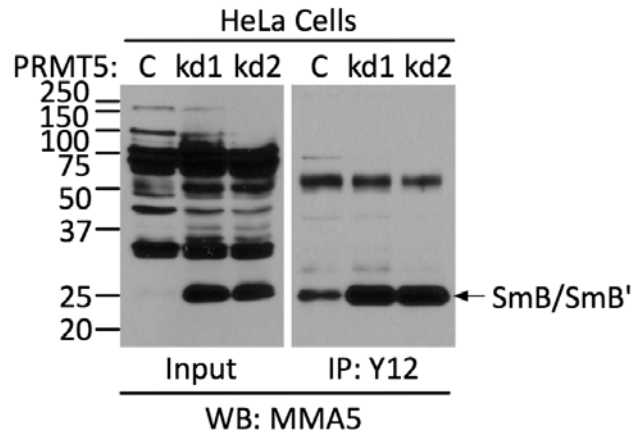


Figure S4. Workflow for the two-dimensional quantification of MMA, ADMA, SDMA, and arginine in MEFs.

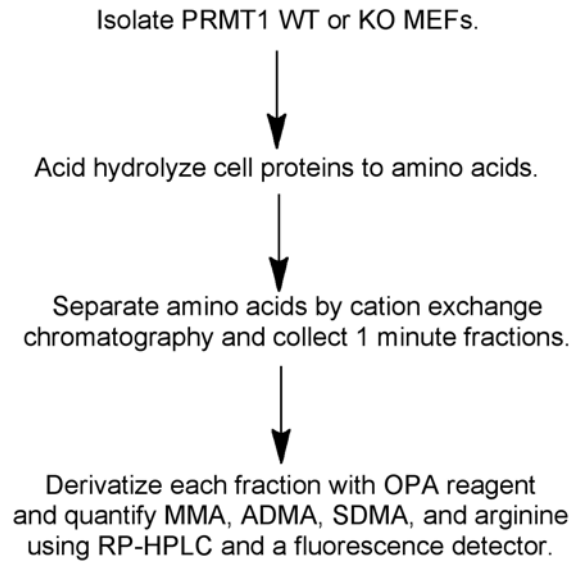


Figure S5. Reverse-phase HPLC methods optimized to quantify OPA-derivatives of arginine (R), MMA, ADMA, and SDMA.

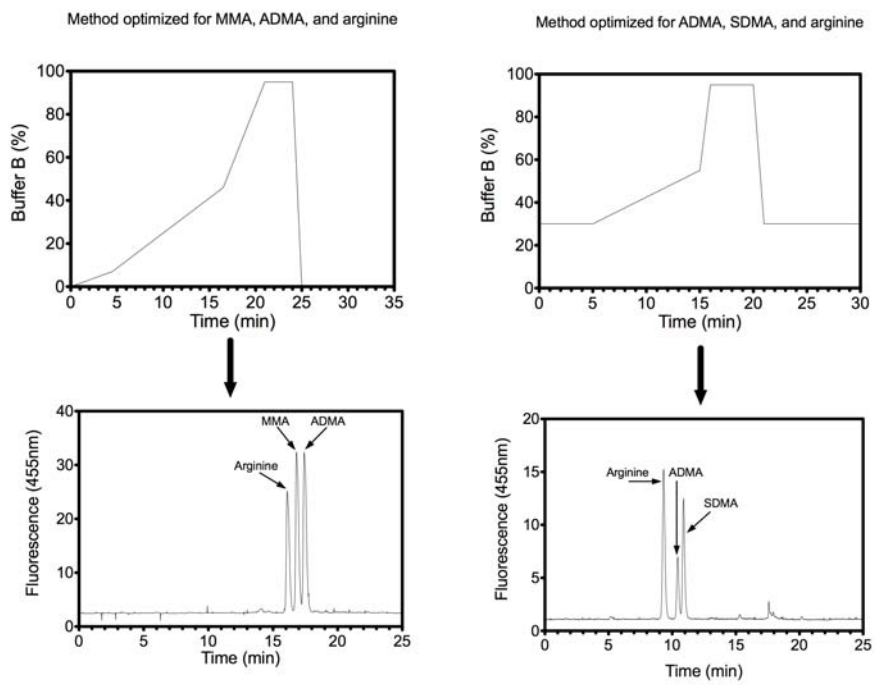


Table S1. Comparison of the relative levels of MMA, ADMA, and SDMA in different mammalian cells. Values from rat brain and liver were taken from Matsuoka (1972)¹ as translated by Paik and Kim (1980)², and converted from μ mol per g protein assuming an average arginine residue content of 5% in proteins.

Cells	MMA	ADMA	SDMA	Reference
	Average number of residues per 1000 arginine residues			
Wild-type MEFs	0.12	4.01	0.34	This study
PRMT1 KO MEFs	0.57	2.13	0.94	This study
Rat brain	2.04	3.60	0.99	1, 2
Rat liver	0.65	2.95	0.35	1, 2
Rat brain nuclear fraction	1.98	10.1	1.10	1, 2

1. Matsuoka, M. [Epsilon-N-methylated lysine and guanidine-N-methylated arginine of proteins. 3. Presence and distribution in nature and mammals]. *Seikagaku* **44**, 364-70 (1972).
2. Paik, W.K. & Kim, S. Natural occurrence of various methylated amino acid derivatives. (ed. Meister, A.) (John Wiley & sons, New York, 1980).

Table S2. Antibodies used in this study. The monomethylarginine (MMA1-5), asymmetric dimethylarginine (ADMA) and symmetric dimethylarginine (SDMA) antibodies tested in this study were generated by Cell Signaling Technology®.

Antibody Name	Company	Antibody #	Catalog #	Antibody type	Host Species	WB Dilution	Results Location
MMA1	Cell Signaling	D5A12A3	8711	Monoclonal	Rabbit	1:2000	Figure 1A-E
MMA2	Cell Signaling	D3C4A6	8015	Monoclonal	Rabbit	1:1000	Figure 1A-E Figure 2A Figure S1
MMA3	Cell Signaling	D2F4E5		Monoclonal	Rabbit	1:1000	Figure 1A-E
MMA4	Cell Signaling	D1C6D1		Monoclonal	Rabbit	1:1000	Figure 1A-E
MMA5	Cell Signaling	D7B7F1		Monoclonal	Rabbit	1:1000	Figure 1A-E Figure S3
ADMA	Cell Signaling	BL8241	Not yet commercially released	Polyclonal	Rabbit	1:500	Figure 1A-E Figure 2B
SDMA	Cell Signaling	BL8243	Not yet commercially released	Polyclonal	Rabbit	1:1000	Figure 1A-E Figure 2C
H3R17me2a	Millipore	N/A	07-214	Polyclonal	Rabbit	1:1000	Figure 1A-E
Y12	A gift from Robin Reed	N/A	N/A	Monoclonal	Mouse	1:100	Figure S3
PRMT1	A gift from Stephane Richard	N/A	N/A	Polyclonal	Rabbit	1:1000	Figure 1A Figure 2 Figure S1 Figure S2A-B
PRMT3	N/A	N/A	N/A	Polyclonal	Rabbit	1:500	Figure 1B Figure S1
CARM1	Bethyl	N/A	A300-421A	Polyclonal	Rabbit	1:2000	Figure 1C Figure S1
PRMT5	Active Motif	N/A	61001	Polyclonal	Rabbit	1:2000	Figure 1D Figure S1
PRMT6	Bethyl	N/A	A300-929A	Polyclonal	Rabbit	1:1000	Figure 1E Figure S1
PRMT7	A gift from Said Sif	N/A	N/A	Polyclonal	Rabbit	1:500	Figure S1